Multiferroic and Ferroic Topological Order in Ligand-Functionalized Germanene and Arsenene

Liangzhi Kou,[1,*] Yandong Ma,[2] Ting Liao,[1] Aijun Du,[1] and Changfeng Chen[3]

[1]*School of Chemistry, Physics and Mechanical Engineering Faculty, Queensland University of Technology, Garden Point Campus, Brisbane, QLD 4001, Australia*

[2]*School of Physics, State Key Laboratory of Crystal Materials, Shandong University, Shandanan Str. 27, 250100 Jinan, People's Republic of China*

[3]*Department of Physics and Astronomy, University of Nevada, Las Vegas, Nevada 89154, USA*

(Received 25 April 2018; revised manuscript received 23 July 2018; published 28 August 2018)

Two-dimensional (2D) materials that exhibit ferroelectric, ferromagnetic, or topological order have been a major focal topic of nanomaterials research in recent years. The latest efforts in this field explore 2D quantum materials that host multiferroic or concurrent ferroic and topological order. We present a computational discovery of multiferroic state with coexisting ferroelectric and ferromagnetic order in recently synthesized CH_2OCH_3-functionalized germanene. We show that an electric-field-induced rotation of the ligand CH_2OCH_3 molecule can serve as the driving mechanism to switch the electric polarization of the ligand molecule, while unpassivated Ge p_z orbits generate ferromagnetism. Our study also reveals coexisting ferroelectric and topological order in ligand-functionalized arsenene, which possesses a switchable electric polarization and a Dirac transport channel. These findings offer insights into the fundamental physics underlying these coexisting quantum orders and open avenues for achieving states of matter with multiferroic or ferroic-topological order in 2D-layered materials for innovative memory or logic device implementations.

DOI: 10.1103/PhysRevApplied.10.024043

I. INTRODUCTION

Ferroelectricity is a quantum order characterized by a spontaneous electric polarization that is switchable by an external electric field, and materials possessing this property have been widely exploited for applications in nonvolatile memories, capacitors, actuators, and sensors [1]. Traditionally, studies of ferroelectric materials mainly focus on complex oxides, such as $BaTiO_3$ and $PbTiO_3$, which possess large electronic band gaps that stabilize their spontaneous polarization [2]. However, these traditional ferroelectric materials are often plagued by dangling bonds and depolarization when their thickness is reduced to meet technological demands for device miniaturization; ferroelectricity may even disappear in films below a critical thickness. To resolve this problem, two-dimensional (2D) materials that possess stable ferroelectricity have been actively sought in recent years. Efforts in this area have been greatly facilitated by the rise of a rich variety of 2D materials since the discovery of graphene that has provided an excellent platform for exploiting new quantum orders and physics [3]. In particular, the recent experimental observation of stable in-plane spontaneous polarization in a single-layer atomic-thick SnTe with a ferroelectric transition temperature of 270 K has opened a research avenue for realizing 2D ferroelectricity [4]. Layered semiconducting indium selenide (α-In_2Se_3) was predicted to be a room-temperature out-of-plane polarized ferroelectric down to the single atomic-layer limit (thickness of approximately 1 nm), with an electric dipole of 0.11 eÅ per unit cell [5]. This prediction has been confirmed by recent experiments using scanning transmission electron microscopy and Raman measurements [6,7]. Additional layered materials have been theoretically predicted to possess ferroelectricity. For example, monolayer oxidized MXene (Sc_2CO_2) is shown to host switchable polarization through an intermediate antiferroelectric phase [8]; the family of SnS, SnSe, GeS, and GeSe layers [9], and the 1T phase of MoS_2 are predicted to possess in-plane or out-of-plane ferroelectricity with low-switch energy barriers [10]. Ferroelectricity also has been proposed in bismuth oxychalcogenides [11], bilayer materials (such as BN, GaSe) with different stackings [12], and chemically functionalized phosphorene [13].

Ferromagnetism in 2D materials has also been extensively pursued. It can be induced by doping [14], defects [15], or transition-metal decoration in 2D materials [16], such as graphene and transition-metal dichalcongenides. Depending on the electronic properties, these materials can be classified as magnetic metals or semiconductors. For

*kouliangzhi@gmail.com

the first class, which is more commonly seen, magnetism is associated with spin-polarized states crossing the Fermi level, leading to the metallic nature of the system, which excludes the possibility of concurrently hosting ferroelectricity in these ferromagnetic materials. Magnetic semiconductors are rarely observed in 2D limits. It was recently proposed that chemically functionalized phosphorene may harbor coexisting ferromagnetism and ferroelectricity [13], but it is challenging to precisely functionalize the target material to control these quantum orders. Very recently, two truly 2D semiconducting magnets, CrI_3 [17,18] and $CrGeTe_3$ [19], were experimentally created, and these works have laid an important foundation for exploring 2D magnetic materials for memory storage and spintronics applications [20].

We present a computational discovery based on first-principles calculations that demonstrate coexisting ferroelectricity and ferromagnetism in ligand-functionalized 2D germanene, which was recently synthesized in experiment. The in-plane ferroelectric switch can be driven by a rotation of the polarized ligand CH_2OCH_3 molecule with a low (0.1 eV) kinetic barrier. The ferromagnetism in the system, with a magnetic moment of 1 μ_B per atom, is generated by the unoccupied p_z orbits on the Ge sites not functionalized by the ligand group. We further explored a similarly structured CH_2OCH_3-functionalized arsenene, which may be synthesized using the same experimental approach. Our results reveal an interesting coexistence of topological order and in-plane ferroelectricity that can be tuned by rotating the polarized functional group. We propose to use an in-plane electric field from a suitably selected substrate such as hexagonal boron nitride to control the ferroelectric switch. The discovery of coexisting ferroelectricity, ferromagnetism, and/or topological order in functionalized 2D materials opens avenues for nonvolatile memory storage and spintronic applications.

II. COMPUTATIONAL METHODS

Structural relaxation and electronic structure calculations are carried out using first-principles methods based on the density-functional theory (DFT) as implemented in the Vienna Ab Initio Simulation (VASP) package [21]. The generalized gradient approximation (GGA) in the Perdew–Burke–Ernzerhof (PBE) [22,23] form for the exchange and correlation potential, together with the projector-augmented wave (PAW) method, are adopted. The structural models for ligand-functionalized germanene and arsenene are periodic in the x–y plane and are separated by at least 10 Å along the z direction to avoid interactions between adjacent layers. All atoms in the unit cell are fully relaxed until the force on each atom is less than 0.01 eV Å^{-1}. The Brillouin-zone integration is sampled by $9 \times 9 \times 1$ k-grid mesh for a unit cell, producing good convergence in calculated total energy. An energy cutoff of 400 eV is chosen for the planewave basis. The van der Waals (vdWs) interaction is introduced, as described by a semiempirical correction using the Grimme method (DFT-D3) [22]. Spin-orbit coupling is included at the second variational step using scalar-relativistic eigenfunctions as the basis. The macroscopic electronic polarization of the system is calculated within the Berry phase method [24,25], which includes ionic and electronic contributions. Energy barriers for phase transitions are calculated using the climbing-image nudge elastic band (CI NEB) method as implemented in the VASP transition state tools [26].

III. RESULTS AND DISCUSSION

Germanene is a single atomic layer of Ge atoms arranged in a honeycomb hexagonal lattice akin to graphene, but with out-plane buckling due to the weak π-π orbital overlap. This structure was first theoretically proposed [27], and was recently synthesized by experiment on various metal substrates, including Ag [28], Au and Pt [29], and Al (111) surfaces [30]. Germanene is unstable in air, but this problem can be effectively addressed by ligand functionalization. For example, methyl-terminated [31] or hydrogen-passivated [32] germanene shows improved stability and can be fabricated and exfoliated into single atomic layers. Recently, Jiang *et al*. [33] reported synthesis of functionalized germanene with ligand groups ($-CH_2OCH_3$, $-CH_2CH_2$ or $CH_2CH{=}CH_2$), which possess good stability and interesting electronic properties. The electric polarization of these ligand groups offers an excellent platform to explore 2D ferroelectricity.

We construct a structural model of CH_2OCH_3-functionalized germanene, shown in Figs. 1(a) and 1(b), to represent the experimentally synthesized system [32], where the Ge atoms adopt a stable sp^3 bonding state, as in recently produced methyl-functionalized germanene [31], and the chemical functional groups bond on both sides of the germanene layer. A structural asymmetry of the ligand CH_2OCH_3 molecule produces a spontaneous electric polarization in the system. We first arrange the ligand such that the molecules on the two sides of the germanene layer are pointed in opposite directions. The spontaneous electric polarizations of the ligand molecules on the two sides counteract, thereby creating a paraelectric state that possesses an inversion symmetry described by the point group S_2. The energetic calculations show that the system in such a structural arrangement is stable with the lowest total energy as shown in Fig. 2(a). This structure has a lattice constant of 4.19 Å and possesses a slight buckling along the thickness direction. The C atom of the CH_2O part in ligand CH_2OCH_3 is located on top of the Ge atom while the C atom of the CH_3 part is on top of the O atom. To check the electronic properties of the fully functionalized germanene, we calculated the corresponding band structures and found that it is a semiconductor

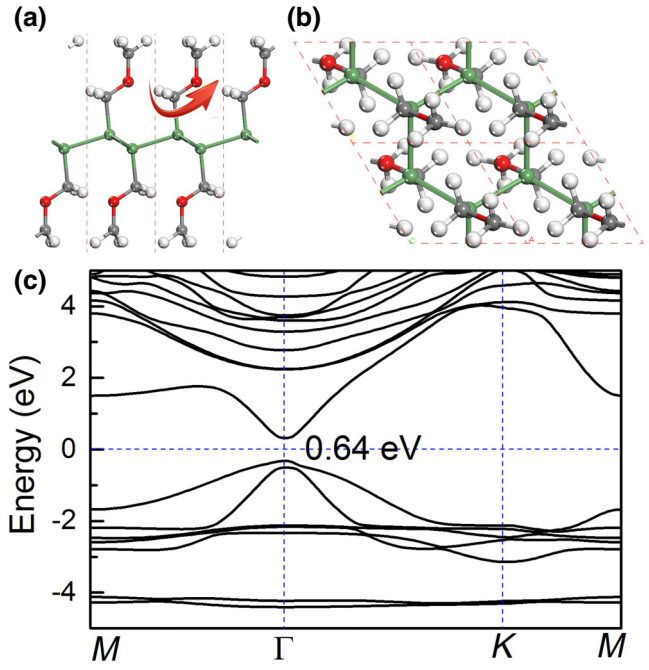

FIG. 1. (a) Side and (b) top views of the structural model for CH_2OCH_3-functionalized germanene layer, where the cyan, gray, red, and white balls represent Ge, C, O, and H atoms, respectively; the red dashed lines highlight the unit cell used in the present work, and the red arrow in (a) indicates the rotation direction of the ligand molecules. (c) The electronic band structure of functionalized germanene.

with a direct gap of 0.64 eV at the Γ point. This relatively large band gap plays an essential role in ensuring the stability of the spontaneous polarization and, therefore, avoiding any appreciable depolarization during the field-induced ferroelectric switch as will be discussed below.

A change in the configuration of the ligand molecules away from their symmetric positions creates an in-plane electric polarization, whose magnitude and direction are dependent on the relative position of these molecules. This property can be exploited to achieve ferroelectric switch. To verify this prediction, we rotate the CH_2OCH_3 molecules on one (top) side of the germanene layer as indicated in Fig. 1(a) to evaluate the energy barriers and check the evolution of the polarization direction and magnitude. We find several stable configurations that possess similar total energy as the symmetric configuration as shown in Fig. 2. The paraelectric phase with the inversion symmetry [configuration I, Fig. 2(b)] has the lowest total energy. When the molecules are rotated, the total energy of the system increases gradually up to a rotation angle of about 30° and then decreases; at about 60° rotation, the system reaches another stable phase [configuration II], which has almost the same total energy as that of configuration I, after overcoming an energy barrier of 0.12 eV/unit cell. Additional rotations of 60° and 120° turn the system into the third and fourth stable phases, i.e., configurations III and IV, respectively, with the corresponding energy barriers of 0.07 and 0.09 eV/unit cell. The ligand rotation changes the direction of the spontaneous electric polarization, as indicated by the blue arrows in Fig. 2(b). We have calculated the polarization based on the Berry-phase theory, and found that the out-of-plane polarization is less affected by the ligand rotation, while the in-plane value is significantly modulated. Due to the offset from the two sides, the net in-plane polarization is zero for configuration I. The magnitude of the polarization increases with the rotation, as shown in Fig. 2(c). At 60° rotation, the spontaneous polarizations along the x and y directions, denoted as P_x and P_y, respectively, are -0.11×10^{-10} and 0.57×10^{-10} C/m. With further increasing rotation, the value of P_y reaches the maximum at around 90° and then decreases to zero at 180°; subsequent rotations reverse the polarization direction. Meanwhile, P_x remains negative and its magnitude keeps increasing to -0.8×10^{-10} C/m up to 180° rotation; any further increased rotation angle reduces the magnitude of the polarization and eventually returns it to zero without any polarization direction reversion. These results indicate that an in-plane ferroelectricity can be achieved in ligand-functionalized germanene, which is driven by a ligand rotation mechanism.

During surface functionalization of germanene, it is inevitable that some of the sites fail to bond with ligand molecules, and it is easier to functionalize only one side of the 2D layer while the other side is undecorated and couples to a substrate, as has been demonstrated in the half-passivated graphene [34]. Such unpassivated localized and unpaired electrons may induce magnetism in the system [15,34]. Here we explore possible ferromagnetism induced by the nonbonding Ge sites. To avoid local distortion, we build a 2×2 supercell and chose two unpassivated sites at opposite locations on a Ge hexagonal lattice, with one top and one bottom CH_2OCH_3 molecule removed as shown in Fig. 3(a). From a density-of-state analysis shown in Fig. 3(b), the spin-up and spin-down states are unequal near the Fermi level, indicating that a ferromagnetic state is indeed generated by the missing functionalization at the two Ge sites. The system is a magnetic semiconductor as there is no state crossing the Fermi level. Calculated spin density distribution in the inset of Fig. 3(b) shows a localized magnetic moment of 1 μ_B on each unpassivated Ge atom. It is noted, however, that the ferromagnetic state is only 1 meV lower in energy than the antiferromagnetic state, which means the ferromagnetism is only stable in low-temperature environments. From the projected density of states in Fig. 3(d), one can see that the magnetism mainly stems from the p_z orbit of the unpassivated Ge atoms. We also consider the case with only one side of the germanene layer passivated with CH_2OCH_3 molecules, and obtain the same results, namely a localized magnetic moment of 1 μ_B at each unpassivated Ge site stemming

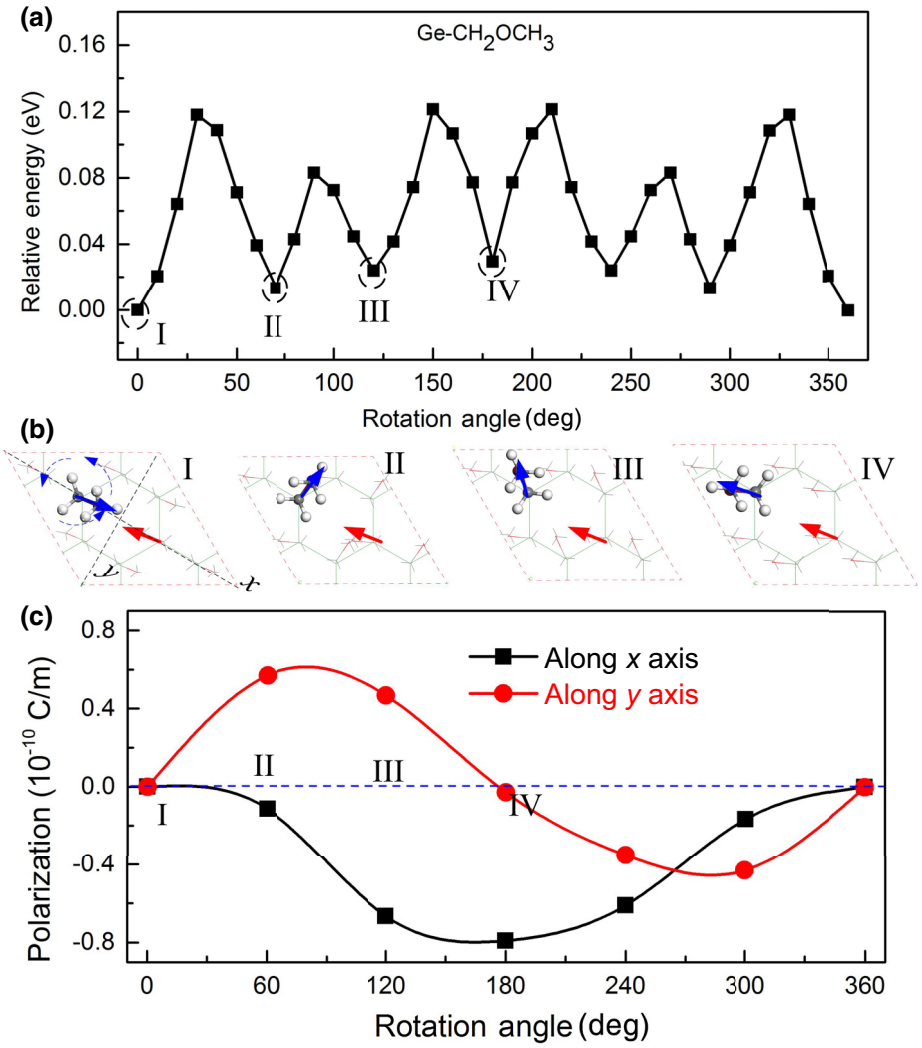

FIG. 2. (a) Energy variation and kinetic barrier of ligand molecule rotation. Four stable configurations are labelled as I, II, III, and IV. (b) The configurations of the four stable structures indicated in (a); for clarity, only the atoms in the rotating CH_2OCH_3 molecule on the top surface are shown, while all other atoms and bonds are represented by lines. The red and blue arrows indicate the polarization directions of the CH_2OCH_3 molecule on the bottom (without rotation) and top (with rotation) surfaces, respectively. (c) Variation of the polarization along the x and y directions [as indicated in (b)] when the CH_2OCH_3 molecule rotates; the polarization direction along the y axis reverses, achieving in-plane ferroelectricity.

from the p_z orbit of the Ge atom, and the system is in a semiconducting state. Moreover, when ligand CH_2OCH_3 molecules on the top surface are rotated, the direction of the in-plane electric polarization changes and reverses, achieving in-plane ferroelectricity [Figs. 3(c) and 3(d)].

The in-plane ferroelectricity driven by ligand molecules is expected to be a more general phenomenon in 2D-layered materials beyond the functionalized germanene. We have examined a 2D arsenic layer, also known as arsenene, which has been theoretically proposed [35]. It becomes a topological insulator exhibiting the quantum spin Hall effect when surface functionalized with H [35], F, OH, and CH_3 [36]. Based on the successful functionalization of germanene [33], we studied the passivation of CH_2OCH_3 on arsenene as a theoretical model to explore the possible coexistence of ferroelectricity and topological order. The fully relaxed structure of CH_2OCH_3 functionalized arsenene is shown as the inset in Fig. 4(a). Similar to the germanene case, the paraelectric phase with inversion symmetry for the ligand arrangement has the lowest total energy. Slightly different from CH_2OCH_3-functionalized germanene, the relaxed structure of arsenene is flat without any out-of-plane buckling, and the lattice constant is 4.901 Å. Similar to AsX (X=H, F, OH or CH_3) [36,37], CH_2OCH_3-functionalized arsenene is a semimetal with a Dirac cone at the K point of the Brillouin zone when spin orbit coupling (SOC) is not considered, but an appreciable gap (0.1 eV) is opened when the SOC is turned on, see Fig. 4(c). The system is in a topologically nontrivial phase, as confirmed by explicit topological invariant index Z_2 calculations using the code Z_2 pack [38,39]. The topological phase and nontrivial band gap are robust and well preserved when ligand CH_2OCH_3 molecules are rotated. For example, the non-SOC Dirac cone at the K point is retained when ligand molecules are rotated by 120°. The band states are slightly split induced by the out-of-plane symmetry breaking, see Fig. 4(d), but the semiconducting nature and the topological phase are well preserved, providing an excellent platform to study 2D materials with coexisting ferroelectricity and topological order.

Following the same procedure outlined above for CH_2OCH_3-functionalized germanene, we rotate the polar

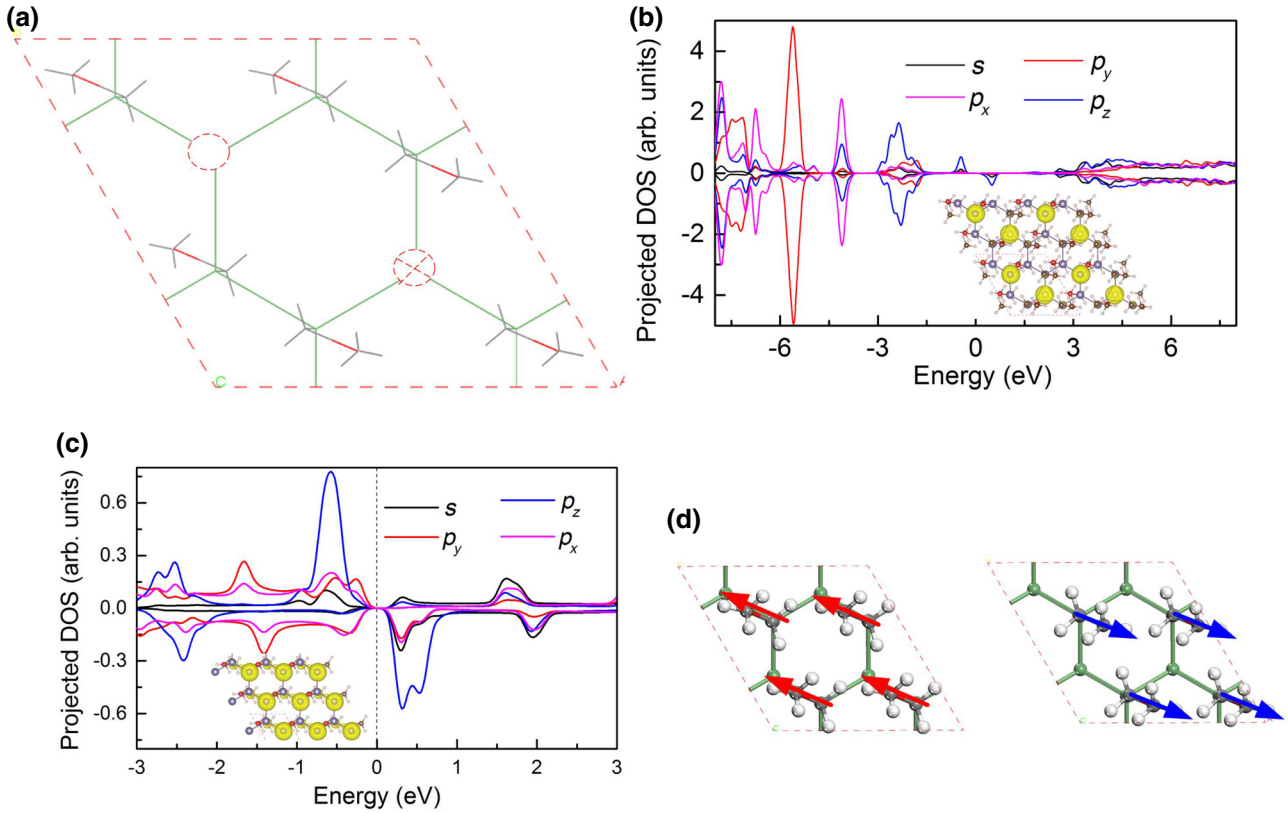

FIG. 3. (a) Partial functionalization of the germanene layer; the dashed circles represent the unpassivated Ge atoms. (b) Orbitally resolved density of states for Ge, which clearly shows that the magnetism stems from the unoccupied p_z orbit of the Ge atoms, the inset shows the spatial spin density distribution with an isosurface of 5×10^{-3} e/Å^3. Electronic properties and polarization direction of half-passivated germanene by ligand CH_2OCH_3. (c) Projected electronic density of states (DOS) for Ge atoms of half-passivated germanene by ligand CH_2OCH_3; the inset shows the corresponding spin distribution. (d) Polarization (directions indicated by the arrows) reversal when ligand CH_2OCH_3 molecules are rotated by 180°.

ligand on one side of the functionalized arsenene to examine the direction change of the polarization and subsequent in-plane ferroelectricity. Similar to the situation in functionalized germanene, there are multiple (three) stable configurations at different rotation angles due to the special relative position of CH_2O sitting on top of an As atom [the C—O bond is collinear with the Ge—Ge bond as seen from the top view in the inset of Fig. 4(a)]. The three stable configurations occur at the rotation angles of 0°, 120°, and 240°, respectively. The energy barrier between these three stable configurations is calculated to be around 0.1 eV. As a result of the polarization direction change of CH_2OCH_3, the in-plane polarization along the x and y directions is changed. At increasing rotation angles, the polarization magnitude along the x direction increases until the angle rises to about 200°, reaching the maximum polarization of 0.42×10^{-10} C/m, then decreases at further increasing angles, returning to zero after a full round of rotation. The polarization direction remains unchanged during this entire process, rendering no ferroelectric switch along this direction. In contrast, the polarization along the y direction is reversed after the ligand CH_2OCH_3 is rotated past 240°, thus realizing the in-plane ferroelectricity. It is seen that the polarization variation along the y direction under the ligand rotation in functionalized arsenene is not symmetric relative to the rotation angle of 180°. This is because, unlike the CH_2OCH_3-functionalized germanene which is stable at the rotation of 180° [see configuration IV in Fig. 2(b)], functionalized arsenene at 180° ligand rotation is in a high energetic state, see Fig. 4(a), and the ensuing structural relaxation leads to a rearrangement of the ligands, producing a non-zero polarization along the y direction and, therefore, the asymmetric polarization curve as shown in Fig. 4(b). Despite the difference in such structural and polarization details, a 2D in-plane ferroelectricity is achieved in the functionalized arsenene, demonstrating the coexistence of ferroelectric and topological order in this system.

We finally discuss a feasible means for achieving an effective control of the ligand molecule rotation to tune the electric polarization. Depicted in Fig. 5(a) is a model setup of functionalized germanene placed on top of a substrate of

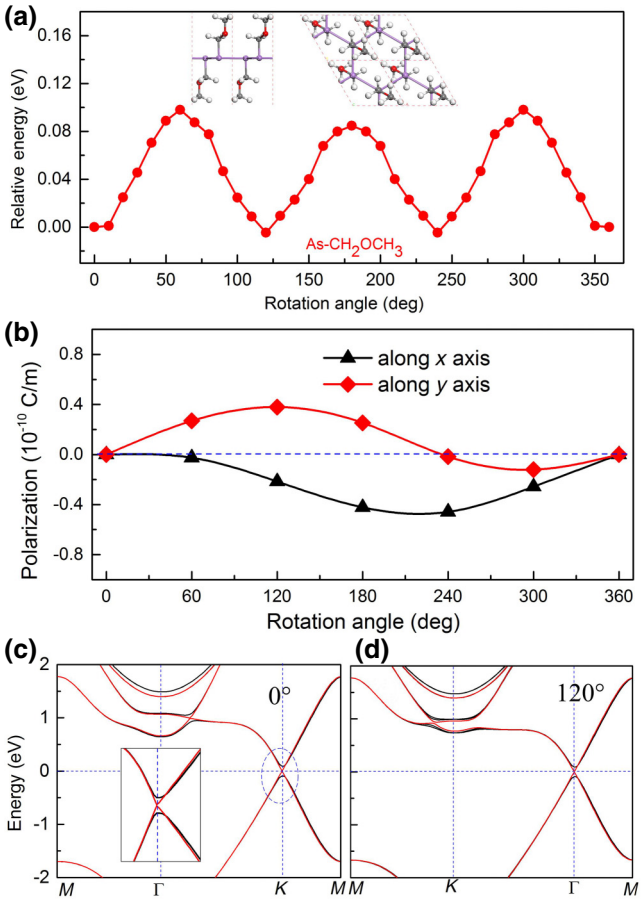

FIG. 4. (a) Energy variation and kinetic barrier for CH_2OCH_3 rotations in functionalized arsenene; the insets show the structural models. (b) Variation of the polarization along the x and y directions. (c),(d) Electronic band structures of the symmetric ligand configuration with the rotation angle of 0° and the asymmetric ligand configuration with the rotation angle of 120°. The topological order is preserved under the ligand rotation, although there is a band splitting due to an out-of-plane symmetry breaking.

hexagonal BN, which is chosen for a good lattice matchup (3×3 Ge-CH_2OCH_3 on top of 5×5 BN; other appropriate substrates may also be used). The ligand molecules at the bottom of the functionalized germanene layer bond to the BN substrate through a vdWs interaction, which is not very strong but is sufficient to hold the system in place. When an in-plane electric field is applied, the bottom ligand layer in direct contact with the substrate remains fixed, while the polarization direction of the CH_2OCH_3 molecules in the top layer on the free side will be modulated due to the nonuniform force distribution induced by the electric field relative to the bonded Ge atoms. It should be noted that the effect of an in-plane electric field on the ligand molecules cannot be simulated in the present calculations since the studied objects are 2D-layered materials with periodic boundary conditions. The current discussions are based on

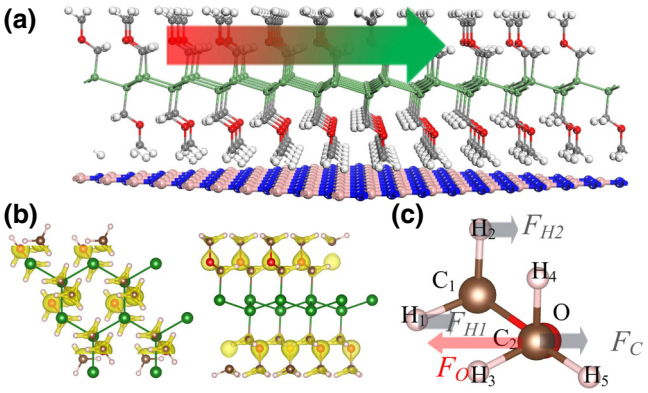

FIG. 5. (a) A schematic diagram of the electric-field-induced ligand rotation. (b) Charge distributions on the ligand molecule CH_2OCH_3 and (c) the associated force analysis.

an analysis of perspectives on polarizability, which serves a useful purpose for understanding experiments since an in-plane electric field can be applied across the synthesized Ge-CH_2OCH_3 nanoflakes or ribbons. A Bader charge analysis shows that the C atom (C_2) of the CH_3 part of the ligand CH_2OCH_3 molecule that is located on top of the O atom possesses a net charge of $+0.07e$ and the O atom possesses a charge of $-1.02e$, while the electron distribution on the H atoms are small (about $0.05e$) and uniform, see Fig. 5(b). As a result, an in-plane electric field as indicated in Fig. 5(a) produces a much larger electrostatic force on the O atom (F_O) than that (F_C) on the C atom of CH_3, and the two forces are in opposite directions as indicated by the arrows in Fig. 5(b) due to the opposite charges. These forces produce a torque around the C_1 site, which is covalently bonded to the Ge atom, serves as a strong anchor, and generates a rotation of the ligand molecule, switching the polarization direction of the CH_2OCH_3 molecule. Based on our calculated kinetic barrier of about 0.1 eV for the rotation [see Fig. 2(a)], it is estimated that the required critical in-plane electric field to achieve the ligand rotation is 0.07 V/Å. This analysis is consistent with previous work on molecular rotation in static and dynamic electric fields from the perspective of polarizability [40]. Electric-field-controlled polarization rotation has been demonstrated in a dipole azimuthal 3-chloroprop-1ynyl on the surface of quartz glass driven by an electric field [41] and a dipole molecule in a homogeneous electric field [42]. Since substrate-supported CH_2OCH_3-functionalized germanene has been experimentally synthesized, it is highly feasible to verify the predicted electric-field-induced molecular rotation and the resulting ferroelectricity.

The total energies of the symmetrical or rotated configurations [see Figs. 2(a), (2b) and 4(a)] are quite close to each other, with differences of only several or tens of meV, which means that the ligand molecules of as-synthesized Ge-CH_2OCH_3 may not be orderly arranged as shown in Figs. 1 and 2. However, an applied in-plane electric field

will regularize the orientations of polarized CH_2OCH_3 as discussed above, leading to the orderly arranged functionalization and ferroelectric switch.

The controllable in-plane ferroelectricity with applied electric field will find wide applications in memory or logical device designs. Taking the functionalized germanene as an example, it has six stable configurations with the lowest total energies as shown in Fig. 2(a) when the ligand CH_2OCH_3 on the top surface is fully rotated, which can be achieved with the controllable direction of an applied electric field (Fig. 5). Based on the direction of ferroelectricity, it can be classified as two types, positive and negative. We can thus propose the binary data storage prototype if defining the positive in-plane ferroelectricity as logic 1 while the negative one is 0. The data writing of logic 1 can be achieved via applying an electric field which has a direction angle of 30°–120° relative to the CH_2OCH_3 shown in Fig. 2(b). After the applied external electric field is removed, the ferroelectric domain will be automatically relaxed to configuration II or III due to the lowest total energy. It thus has positive ferroelectricity (logic 1) and achieves innovative storage. Similarly, the logic 0 (negative ferroelectricity) can be written with an electric field of 150°–330°. The data can be read by measuring the direction of ferroelectricity. As the ferroelectric direction is controlled by the ligand molecule, the storage density can be quite high in the prototype as the information bit can be directly related to one ligand arrangement. Coupled with ferromagnetism or quantum spin Hall effect in these 2D materials as revealed above, the device of innovative memory can be integrated with quantum computation and dissipationless transport at the edge, designing high-performance devices with high storage density, high speed, and low heat dissipation.

In conclusion, our computational study has unveiled a 2D multiferroic state with coexisting ferroelectric and ferromagnetic order in recently synthesized ligand CH_2OCH_3-functionalized germanene. We have identified by first-principles calculations the fundamental underlying mechanisms, i.e., a field-induced ligand molecule rotation for driving the electric polarization reversal and a spin-polarized charge distribution on unpassivated Ge sites for producing the ferromagnetism. Moreover, we find in similarly functionalized arsenene concurrent ferroelectric and topological order. The present findings of multiple coexisting quantum orders in functionalized atomic thin layers highlight a promising route to developing a large class of 2D materials for nanoscale electronic and spintronic applications.

ACKNOWLEDGMENTS

We acknowledge support from the high-performance computing facility at the Queensland University of Technology, the Pawsey Supercomputing Centre and Australian National Facility. Financial support by the ARC Discovery Early Career Researcher Grant (No. DE150101854) is gratefully acknowledged.

[1] L. W. Martin and A. M. Rappe, Thin-film ferroelectric materials and their applications, Nat. Rev. Mater. **2**, 16087 (2016).
[2] C. Ederer and N. A. Spaldin, Effect of Epitaxial Strain on the Spontaneous Polarization of Thin Film Ferroelectrics, Phys. Rev. Lett. **95**, 257601 (2005).
[3] R. Mas-Balleste, C. Gomez-Navarro, J. Gomez-Herrero, and F. Zamora, 2D materials: To graphene and beyond, Nanoscale **3**, 20 (2011).
[4] K. Chang, *et al.*, Discovery of robust in-plane ferroelectricity in atomic-thick SnTe, Science **353**, 274 (2016).
[5] W. Ding, J. Zhu, Z. Wang, Y. Gao, D. Xiao, Y. Gu, Z. Zhang, and W. Zhu, Prediction of intrinsic two-dimensional ferroelectrics in In2se3 and other III2-VI3 Van Der Waals materials, Nat. Commun. **8**, 14956 (2017).
[6] Y. Zhou, *et al.*, Out-of-plane piezoelectricity and ferroelectricity in layered α-In_2Se_3 nanoflakes, Nano Lett. **17**, 5508 (2017).
[7] C. Cui, *et al.*, Intercorrelated in-plane and out-of-plane ferroelectricity in ultrathin two-dimensional layered semiconductor In_2Se_3, Nano Lett. **18**, 1253 (2018).
[8] A. Chandrasekaran, A. Mishra, and A. K. Singh, Ferroelectricity, antiferroelectricity, and ultrathin 2D electron/hole gas in multifunctional monolayer MXene, Nano Lett. **17**, 3290 (2017).
[9] M. Wu and X. C. Zeng, Intrinsic ferroelasticity and/or multiferroicity in two-dimensional phosphorene and phosphorene analogues, Nano Lett. **16**, 3236 (2016).
[10] S. N. Shirodkar and U. V. Waghmare, Emergence of Ferroelectricity at a Metal-Semiconductor Transition in a 1 T Monolayer of MoS_2, Phys. Rev. Lett. **112**, 157601 (2014).
[11] M. Wu and X. C. Zeng, Bismuth oxychalcogenides: A new class of ferroelectric/ferroelastic materials with ultra high mobility, Nano Lett. **17**, 6309 (2017).
[12] L. Li and M. Wu, Binary compound bilayer and multilayer with vertical polarizations: Two-dimensional ferroelectrics, multiferroics, and nanogenerators, ACS Nano **11**, 6382 (2017).
[13] Q. Yang, W. Xiong, L. Zhu, G. Gao, and M. Wu, Chemically functionalized phosphorene: Two-dimensional multiferroics with vertical polarization and mobile magnetism, J. Am. Chem. Soc. **139**, 11506 (2017).
[14] N. M. R. Peres, F. Guinea, and A. H. Castro Neto, Coulomb interactions and ferromagnetism in pure and doped graphene, Phys. Rev. B **72**, 174406 (2005).
[15] J. J. Palacios, J. Fernández-Rossier, and L. Brey, Vacancy-induced magnetism in graphene and graphene ribbons, Phys. Rev. B **77**, 195428 (2008).
[16] A. V. Krasheninnikov, P. O. Lehtinen, A. S. Foster, P. Pyykkö, and R. M. Nieminen, Embedding Transition-Metal Atoms in Graphene: Structure, Bonding, and Magnetism, Phys. Rev. Lett. **102**, 126807 (2009).
[17] K. L. Seyler, *et al.*, Ligand-field helical luminescence in a 2D ferromagnetic insulator, Nat. Phys. **14**, 277 (2018).

[18] B. Huang, *et al.*, Layer-dependent ferromagnetism in a van der Waals crystal down to the monolayer limit, Nature **546**, 270 (2017).
[19] C. Gong, *et al.*, Discovery of intrinsic ferromagnetism in two-dimensional van der Waals crystals, Nature **546**, 265 (2017).
[20] C. Huang, Y. Du, H. Wu, H. Xiang, K. Deng, and E. Kan, Prediction of Intrinsic Ferromagnetic Ferroelectricity in a Transition-Metal Halide Monolayer, Phys. Rev. Lett. **120**, 147601 (2018).
[21] G. Kresse and J. Furthmüller, Efficient iterative schemes for *Ab Initio* total-energy calculations using a plane-wave basis set, Phys. Rev. B **54**, 11169 (1996).
[22] S. Grimme, Semiempirical GGA-type density functional constructed with a long-range dispersion correction, J. Comp. Chem. **27**, 1787 (2006).
[23] J. P. Perdew, K. Burke, and M. Ernzerhof, Generalized Gradient Approximation Made Simple, Phys. Rev. Lett. **77**, 3865 (1996).
[24] R. Resta, Polarization as a Berry phase, Europhys. News **28**, 18 (1997).
[25] R. Resta and D. Vanderbilt, in *Physics of Ferroelectrics: A Modern Perspective* (Springer, Berlin, Heidelberg, 2007), pp. 31.
[26] G. Henkelman, A climbing image nudged elastic band method for finding saddle points and minimum energy paths, J. Chem. Phys. **113**, 9901 (2000).
[27] C.-C. Liu, W. Feng, and Y. Yao, Quantum Spin Hall Effect in Silicene and Two-Dimensional Germanium, Phys. Rev. Lett. **107**, 076802 (2011).
[28] M. E. Dávila, L. Xian, S. Cahangirov, A. Rubio, and G. L. Lay, Germanene: A novel two-dimensional germanium allotrope akin to graphene and silicene, New J. Phys. **16**, 095002 (2014).
[29] L. Li, S. Z. Lu, J. Pan, Z. Qin, Y. Q. Wang, Y. Wang, G. Y. Cao, S. Du, and H. J. Gao, Buckled germanene formation on Pt(111), Adv. Mater. **26**, 4820 (2014).
[30] M. Derivaz, D. Dentel, R. Stephan, M.-C. Hanf, A. Mehdaoui, P. Sonnet, and C. Pirri, Continuous germanene layer on Al(111), Nano Lett. **15**, 2510 (2015).
[31] S. Jiang, S. Butler, E. Bianco, O. D. Restrepo, W. Windl, and J. E. Goldberger, Improving the stability and optical properties of germanane via one-step covalent methyl-termination, Nat. Commun. **5**, 3389 (2014).
[32] E. Bianco, S. Butler, S. Jiang, O. D. Restrepo, W. Windl, and J. E. Goldberger, Stability and exfoliation of germanane: A germanium graphane analogue, ACS Nano **7**, 4414 (2013).
[33] S. Jiang, M. Q. Arguilla, N. D. Cultrara, and J. E. Goldberger, Improved topotactic reactions for maximizing organic coverage of methyl germanane, Chem. Mater. **28**, 4735 (2016).
[34] J. Zhou, Q. Wang, Q. Sun, X. S. Chen, Y. Kawazoe, and P. Jena, Ferromagnetism in semihydrogenated graphene sheet, Nano Lett. **9**, 3867 (2009).
[35] S. Zhang, Z. Yan, Y. Li, Z. Chen, and H. Zeng, Atomically thin arsenene and antimonene: Semimetal–semiconductor and indirect–direct band-gap transitions, Angew. Chem. Int. Ed. **54**, 3112 (2015).
[36] J. Zhao, Y. Li, and J. Ma, Quantum spin Hall insulators in functionalized arsenene (AsX, X=F, OH and CH_3) monolayers with pronounced light absorption, Nanoscale **8**, 9657 (2016).
[37] Y.-P. Wang, W.-X. Ji, C.-W. Zhang, P. Li, F. Li, M.-J. Ren, X.-L. Chen, M. Yuan, and P.-J. Wang, Controllable band structure and topological phase transition in two-dimensional hydrogenated arsenene, Sci. Rep. **6**, 20342 (2016).
[38] D. Gresch, G. Autès, O. V. Yazyev, M. Troyer, D. Vanderbilt, B. A. Bernevig, and A. A. Soluyanov, Z2pack: Numerical implementation of hybrid Wannier centers for identifying topological materials, Phys. Rev. B **95**, 075146 (2017).
[39] A. A. Soluyanov and D. Vanderbilt, Computing topological invariants without inversion symmetry, Phys. Rev. B **83**, 235401 (2011).
[40] D. M. Bishop, Molecular vibrational and rotational motion in static and dynamic electric fields, Rev. Mod. Phys. **62**, 343 (1990).
[41] D. Horinek and J. Michl, Molecular dynamics simulation of an electric field driven dipolar molecular rotor attached to a quartz glass surface, J. Am. Chem. Soc. **125**, 11900 (2003).
[42] P. O. F. K. Larsson, Rotation of a rigid diatomic dipole molecule in a homogeneous electric field - II. Energy levels when the field is zero, very weak or very strong, Philos. Trans. R. Soc. London Ser. A **347**, 23 (1994).